FOCUS ISSUE OF SELECTED PAPERS FROM IMLB 2016 WITH INVITED PAPERS CELEBRATING 25 YEARS OF LITHIUM ION BATTERIES

Shedding Light on the Entropy Change Found for the Transition Stage II→Stage I of Li-Ion Storage in Graphite

E. P. M. Leiva,[a,z] E. Perassi,[a] and D. Barraco[b]

[a]*Departamento de Matemática y Física, Facultad de Ciencias Químicas, INFIQC-CONICET, Universidad Nacional de Córdoba, Ciudad Universitaria, Córdoba, Argentina*
[b]*Facultad de Matemática, Astronomía y Física, IFEG-CONICET, Universidad Nacional de Córdoba, Ciudad Universitaria, Córdoba, Argentina*

In order to examine the controversial hypothesis put forward to explain the entropy step experimentally observed for the stage II to stage I transition for lithium intercalation in graphite, a transparent statistical mechanical model is developed. The results obtained show that the entropy increase can be explained by the change of configurational entropy occurring at occupation of half of the lattice. Comparison with experimental data shows that attractive interactions between intercalated particles in the same layer must be assumed, in agreement with the ansatz made in the original experimental work.

Manuscript submitted September 30, 2016; revised manuscript received November 10, 2016. Published November 22, 2016. This was Paper 873 presented at the Chicago, Illinois, Meeting of the IMLB, June 19–24, 2016. *This paper is part of the Focus Issue of Selected Papers from IMLB 2016 with Invited Papers Celebrating 25 Years of Lithium Ion Batteries.*

It is well known that intercalation materials are widely used for electrodes as anodes or cathodes in electrochemical cells to store energy. Materials of intercalation, such as lithium cobalt oxide ($LiCoO_2$),[1,2] lithium iron phosphate ($LiFePO_4$),[3,4] lithium titanate oxide (LTO)[5,6] and graphite,[7,8] are commonly found in electrodes of commercially lithium-ion cells. In addition to the mentioned intercalation materials, there are many others that are currently being studied or used as electrodes in lithium-ion cells. In particular, graphite is the most common material found in anodes of commercial lithium-ion cells.

One of the most important features of the intercalation materials is that they can have ions stored in them with little changes in their crystalline structures. This feature allows a fast ion insertion and extraction and therefore high power density cells can be obtained when used as electrodes. However, a fast ion insertion and extraction generates heat in the cell, which can produce high temperature excursions of the cell and a premature aging.

It has been demonstrated that a great portion of the heat that is generated in the intercalation materials comes from the intercalation entropy during a discharge.[9–11] In this sense, different methods to measure the intercalation entropy have been developed.[12–17] In the case of Li-ion insertion into graphite, the experimental curve for entropy as a function of composition, Reference 12, shows a step in the transition of stage II to stage I that could not be explained in the terms presented there. In a subsequent work,[18] two of the previous authors, state that a possible mechanism of the stage I phase formation may involve a 'dilute lithium layer' (noted dil-Li) that would have an alternating 'normal' Li layer (Li) with a hexagonal structure and a dilute lithium layer following the sequence (Li)–G–(dil–Li)–G. However, in a more recent review, Fultz[19] stated that the vibrational entropy resulting from the insertion dominates the entropy, and also he added that there should be a small change in the configurational entropy when compounds are formed in stage I or II, as they are ordered.

In a previous work[20] we have proposed a theoretical approach to determine the intercalation entropy, and we applied this approach to the graphite/lithium compound. In order to clarify the origin of this entropy, in the present work we have used a simplified two-level lattice gas model to analyze the configurational contribution to the intercalation entropy of the graphite/lithium compound. The main features of the intercalation entropy are elucidated.

[z]E-mail: eze_leiva@yahoo.com.ar

Model and Statistical Mechanical Background

The Monte Carlo simulations performed in Reference 20, based on a semiempirical hamiltonian, showed the sequential filling of a hexagonal lattice in a two-step sequence. Voltammetric experiments also have shown that the occurrence of Stages I and II is related to two well-defined energy states, which become evident as voltammetric peaks. For this reason, and seeking the simplest model that allows the experimental features to be understood, we propose the model described in Figure 1. We show there two lattices, defined as 1 and 2, which we will assume that may be occupied by particles (the Li^+ ions), and we will denote the interaction energies of the particles with the lattices as E_1 and E_2 respectively ($E_1 < E_2$). We will neglect the interactions between particles in different lattices, so that the interaction of the particles coming into lattice 2 with the particles in lattice 1 is included in its energy E_2. Thus, the present formulation corresponds to a two-level lattice gas. It will be assumed that each lattice has M sites where the incoming ions may be located, thus giving a total of $2M$ sites that may be occupied.

In statistical mechanics, all the thermodynamic properties of a system can be obtained from its partition function once it is determined. Different partition functions may be formulated in different ensembles (microcanonical, canonical, grand canonical, etc), depending on the boundary conditions chosen to describe the related thermodynamic systems. However, it can be shown that all the ensembles are thermodynamically equivalent as long as the systems are large enough so that their fluctuations may be ignored.[21] Thus, a currently used strategy

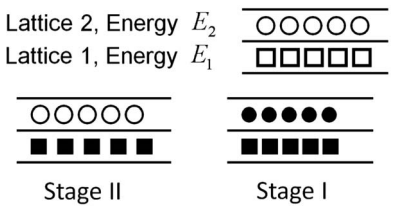

Figure 1. Schematic representation of the present model for Li intercalation in graphite. The upper part shows the two empty lattices (empty symbols), say lattice 1(squares) and lattice 2(circles), which may be progressively occupied by Li ions. The lower part of the figure shows on the left the representation of Stage II (X = 0.5), where filled squares represent filled sites for lattice 1; and on the right, the representation of Stage I (X = 1), where filled circles denote that lattice 2 has also been filled.

is to choose the ensemble where the calculations are less demanding, then calculate the thermodynamic properties within it, and assume the results to be valid for thermodynamic systems under other boundary conditions. This is the approach we have applied here. On this basis, our calculations will be made within the canonical ensemble, where the partition function Q is given by:

$$Q(N, 2M) = \sum_{i(states)} e^{-E_i/kT} = \sum_{j(levels)} \Omega_j e^{-E_j/kT} \quad [1]$$

where Ω_j labels the degeneracy of the j_{th} energy level E_j and N the number of inserted ions. The term $2M$ indicates the total number of sites where the ions may be inserted and kT is the Bolzmann constant multiplied by the absolute temperature.

The degeneracy Ω_i may be straightforwardly calculated by counting the number of ways of distributing N particles among M sites with energy E_1 and M sites with energy E_2. Two cases may by distinguished, for $N < M$ and for $N \geq M$. For $N < M$ we obtain:

$$\Omega_j = \frac{(M!)^2}{(M-N+j)!\,(N-j)!\,(M-j)!\,j!} \quad [2]$$

where j is an index running between 0 and$N$ in Equation 1.

For the case where $N \geq M$ we have:

$$\Omega_j = \frac{(M!)^2}{(2M-N-j)!\,(N-M+j)!\,(M-j)!\,j!} \quad [3]$$

where$j$ is an index running between 0 and $2M - N$ in Equation 1.

The energy for E_j is in turn given by:

$$E_j = \begin{cases} (N-j)E_1 + jE_2 & \text{for } N < M \\ (M-j)E_1 + (N-M+j)E_2 & \text{for } N \geq M \end{cases} \quad [4]$$

We have used a numerical procedure to evaluate the partition function Q for different situations, and found that results with $M = 100$ are converged with respect to the size of the system. Once Q was obtained for different N, different properties were obtained according to following equations:

$$A = -kT \ln Q \quad [5]$$

$$S = -\left(\frac{\partial A}{\partial T}\right)_{M,N} = k\frac{\sum_{j(levels)} \Omega_j \frac{E_j}{kT} e^{-E_j/kT}}{Q} + k \ln Q \quad [6]$$

$$\mu = -kT\left(\frac{\partial \ln Q}{\partial N}\right)_{T,M} \quad [7]$$

$$\left(\frac{\partial N}{\partial \mu}\right)_{T,M} = -\frac{1}{kT}\frac{1}{\left(\frac{\partial^2 \ln Q}{\partial N^2}\right)_{T,M}} \quad [8]$$

where A denotes the Helmholz free energy, S the entropy and μ the chemical potential. The last two equations may be useful to simulate voltammograms under quasi-equilbrium conditions, since μ is linearly related to the electrode potential, and the derivative in Equation 8 is proportional to the current in a linear voltammetric sweep.

Results and Discussion

To proceed with the discussion, instead of using the number of particles as the independent variable, we define the fractional occupation X of the lattices as:

$$X = N/(2M) \quad [9]$$

and all thermodynamic properties will be discussed in terms of this quantity.

Figure 2 shows the entropy of the present system as a function of the occupation, for different energy differences $\Delta E = E_2 - E_1$, which are indicated in the figure.

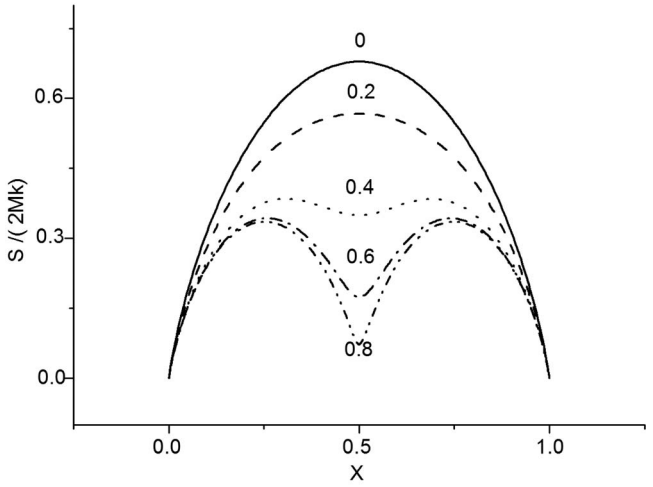

Figure 2. Configurational entropy according to the double lattice model presented in Figure 1, as a function of the fraction of occupied sites X. The entropy has been divided by the total number of lattice sites $2M$, and the energy difference $\Delta E/kT = (E_2 - E_1)/kT$ employed for each curve is shown close by. The $\Delta E/kT$ values were 0 (——), 2 (- - -), 4(· · ·), 6(- · - · - ·) and 8(- · - · - · -) respectively.

Let us discuss first the case $\Delta E = 0$. In this case, the particles distribute over all sites with the same probability, and the entropy reflects the following conditions: for $X \to 0$, we have that $S \to 0$, since there are no particles in the system. In the discrete system, $S(1)/(2Mk) = \frac{\ln(2M)}{2M}$, which comes close to zero for very large systems. For $X \to 1$, we have similarly that $S \to 0$, since the system becomes completely ordered. The entropy maximum occurs at $X = 0.5$, a condition that delivers the maximum number of configurations. It is interesting to see what happens for larger ΔE values. The entropy curve becomes progressively flat at the maximum, and finally develops a local minimum between two local maxima, located at $X \approx 0.25$ and $X \approx 0.75$ (See Figure 2). The derivatives of the curves shown in Figure 2, correspond to the entropy values measured in the literature,[12] and are illustrated in Figure 3. We will from now on denote this quantity as $S'(N) = (\frac{\partial S}{\partial N})_{T,M}$. It is evident from this Figure that a step develops in $S'(N)$ for increasing $\Delta E/kT$ values. The origin of this

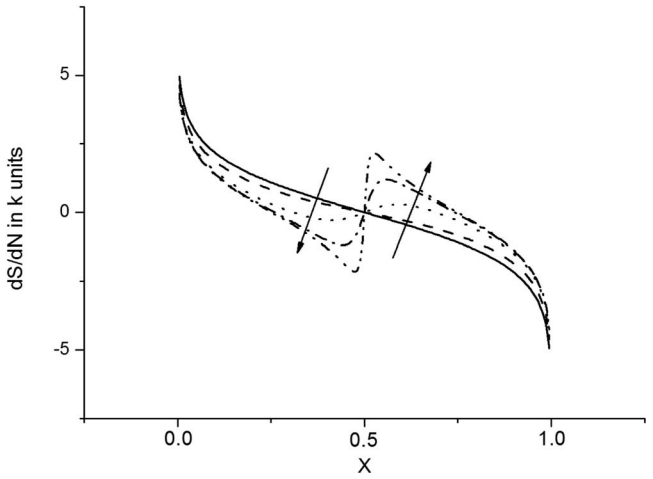

Figure 3. Derivative of the configurational entropy according to the double lattice model presented in Figure 1, as a function of the fraction of occupied sites X. The curves for increasing $\Delta E/kT$ values are indicated by the arrows, and correspond to $\Delta E/kT = 0$ (——), 2 (- - -), 4(· · ·), 6(- · - · - ·) and 8(- · - · - · -), respectively.

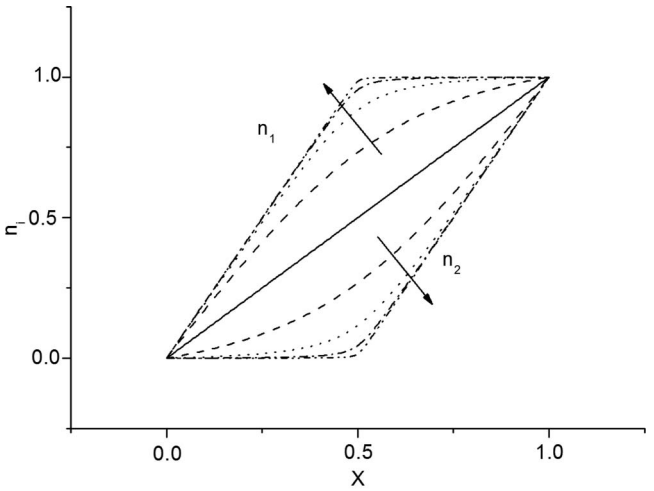

Figure 4. Occupancy n_i of the energy levels E_1 and E_2 as a function of the fraction of occupied sites X, for different energy differences $\Delta E/kT = (E_2 - E_1)/kT$. The $\Delta E/kT$ values correspond to 0 (——), 2 (- - -), 4(· · · ·), 6(- · - · - · -) and 8(- · · - · · -), respectively. The direction of increasing $\Delta E/kT$ values is indicated by the arrows.

step can be understood by consideration of the occupancy of the two energy levels, E_1 and E_2, which are shown in Figure 4.

It becomes evident that as the energy difference $\Delta E/kT$ increases, the occupation of the two energy levels becomes progressively differentiated, until a point is reached where the occupation is close to being sequential. Thus, the situation for $\Delta E/kT = 8$ is such that lattice 1 is practically completed as lattice 2 starts to fill. Under this condition, the step in $S'(N)$ is quite large, since the change in the physical situation is from one where the entropy of the system is rapidly decreasing, as lattice 1 is completely filled, to another one where entropy increases because an empty lattice is starting to be filled. Thus, up to now, the present model is able to account qualitatively for the entropy step found in experiments at $X = 0.5$. However, a close comparison with experiments shows that some improvements are necessary to be able to obtain a quantitative agreement.

If we look, for example, at the voltammograms of Levi et al.,[22] we can see that the peaks attributed to the occurrence of stages I and II are separated by about 37 mV, which in terms of the thermal energy at room temperature (0.0257 eV) amounts to 1.44 kT. Thus, 1.44 is the value that corresponds to $\Delta E/kT$ in the present modeling. Figures 2 and 3 clearly show that such a small value of $\Delta E/kT$ could not account for the step in S' in References 12, 13. In order to come close experimental results, an important conclusion drawn by Levi and Aurbach must be born in mind: The effective interaction of the particles leading to the peaks labeled as e) and d) in Reference 20 is attractive, leading to a half-width of peaks close to 18 mV, instead of the 90 mV for the Langmuirian-Nerstian relationship. These attractive interactions are absent in our model so far, but this can be remediated straightforwardly, by modifying Equation 4 to account for the interaction among particles in an average way. This can be easily done by replacing E_1 and E_2 by E_1^* and E_2^*, which are defined as:

$$E_1^* = E_1 + g_1 N_1^n n_1 \frac{1}{2} \qquad [10]$$

$$E_2^* = E_2 + g_2 N_2^n n_2 \frac{1}{2} \qquad [11]$$

where g_1 and g_2 are interaction parameters, $N_1^n = N_2^n = 6$ is the number of neighbors in each of the lattices, n_1 and n_2 are the occupancies of the layers, and the factor 1/2 is to account for the double summation in the average interaction. The set of Equations 10 and 11 is the Bragg-Williams approximation applied to each of the lattices.[23] Assuming a value of $\Delta E/kT = 1.44$, as suggested by experiments,

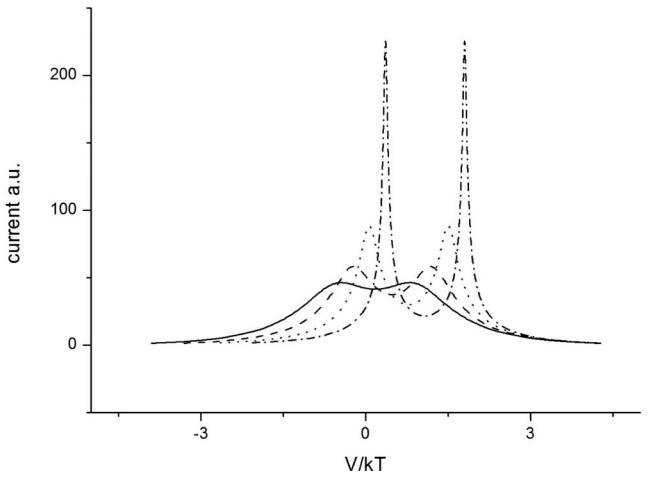

Figure 5. Voltammograms simulated with different values of $g_1 = g_2$ in Equations 10–11. These correspond to: $g_1/(kT) = -0.30$ (——), $g_1/(kT) = -0.40$ (- - -), $g_1/(kT) = -0.50$ (- - -),$g_1/(kT) = -0.60$ (- - -).

we can simulate voltammograms using Equations 7 and 8. Voltammograms simulated with different values of $g_1 = g_2 = g$ are shown in Figure 5, where we can appreciate how the half-width peak is strongly sensitive to the interaction parameter g_i.

According to these results, one possible approach to come closer to experimental findings would be to fit the half-peak width of the experimental voltammograns (18 mV) and calculate with these parameters the $S'(N)$ plots. Calculations with $g/(kT) = -0.471$ deliver a half peak width of this order, and the corresponding $S'(N)$ vs N plot is shown in Figure 6. While the general behavior of the $S'(N)$ - N resembles the experiment, the entropy increases at the transition between stages, say $\Delta S'(II \rightarrow I)$ yields a value 5.8 J/(mol.K), which strongly underestimates the experimental value (14 J/(mol.K)).

While this disagreement may be attributed to the approximate nature of the present model, a number of considerations must be made concerning the experimental results. On the one hand, although the voltammetric experiments have been made at very low sweep rates ($4\mu V.s^{-1}$), it is possible that quasi-equilibrium conditions have not been reached. The potential difference between the anodic and cathodic peaks, as well as their different widths may be an indication of this. Also, it is intrinsic from experiments that the graphite electrodes are not perfect, and a number of other technical features, such as

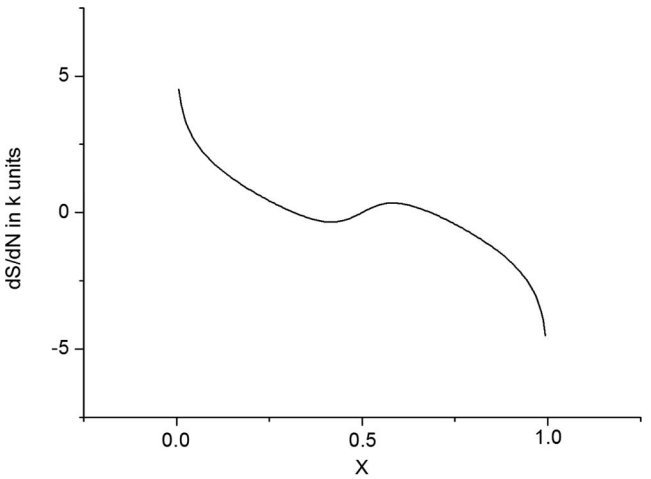

Figure 6. Derivative of the configurational entropy according to the double lattice model presented in Figure 1, as a function of the fraction of occupied sites X for $\Delta E/kT = 1.44$ and $g_1/(kT) = -0.471$.

Table I. Entropy increase at the transition between stages, $\Delta S'(II \rightarrow I)$, for the different values of the interaction parameters g. The predicted voltammetric half peak is also included.

Interaction parameter $g/(kT)$	Entropy change at the stage II→stage I transition $S'(N)$ J mol^{-1} K^{-1}	Voltammetric Half peak width mV
−0.5	7.2	14.1
−0.6	12.6	3.51
−0.65	15.1	0.26
−2/3 (Braggs Williams limit for the first-order phase transition)	15.9	0

contact resistances between grains may be widening the voltammetric profiles. Another consideration that should be taken into account is: the occurrence of borders of the growing phases, suggesting nucleation and growth processes taking place, and also suggesting the occurrence of a first-order phase transition for each of the states being formed (II, I, etc.). It is well known that the incidence of a first order phase transition should be present as a step in the adsorption isotherm, or, what is equivalent, as the occurrence of a *spike* in the voltammogram. Although the latter event has so far not been observed for the present system (probably due to kinetic hindrances, as pointed out above), we will now analyze the occurrence of a first order phase transition within the present modeling.

Depending on the interaction between the particles of the system, the Braggs-Williams approximation predicts an undulation in the pressure-volume isotherms, with the concomitant prediction of a first order phase transition.

Within the present notation, for each of the lattices, the first order phase transition should occur when $g/(kT) = -2/3 = -0.666$. To analyze how the approach to this limit affects the entropy increase at the transition between stages, $\Delta S'(II \rightarrow I)$, we calculated the latter quantity for the different interaction parameters g. These results are shown in Table I.

It is remarkable how the predicted $S'(N)$ values come closer to the experimental results as $g/(kT) \rightarrow -2/3$. The $S'(N)$ vs N for the latter condition is shown in Figure 7.

At first sight, it may appear as strange that interactions between ions that are in the same lattice are attractive, despite having the same charge. However, a couple of considerations are pertinent: Levi and Aurbach[22] have reproduced the voltammetry of the different stages of insertion of Li into graphite. In order to get the half-height widths of the experimental peaks, they must assume attractive interactions among absorbed atoms in the same layers. The theoretical work of Filhol et al.[24] also points in the same direction. These authors performed density functional calculations for the absorption of a neighboring Li atom close to a previously absorbed Li atom. They found that absorption on a second neighboring site is more stable than absorption on more distant sites, clearly denoting an attractive interaction between adsorbates. Thus, it appears that although interactions are repulsive if Li atoms come too close to each other (say first neighbors on the honeycomb graphic lattice), these interactions become attractive if they arrange in a $\sqrt{3} \times \sqrt{3}$ structure.

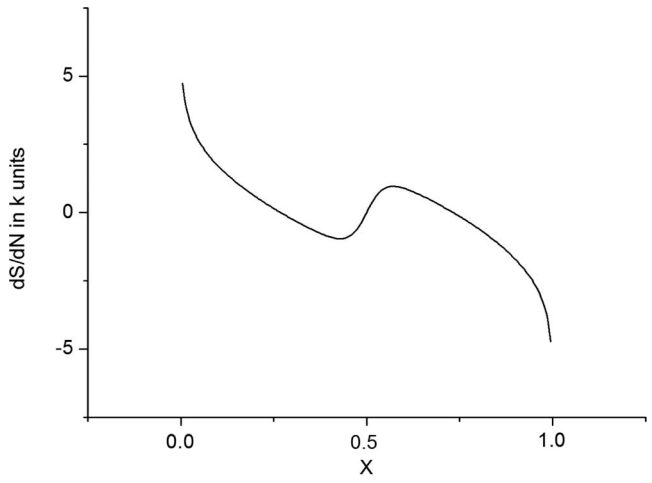

Figure 7. Derivative of the configurational entropy according to the double lattice model presented in Figure 1, as a function of the fraction of occupied sites X for $\Delta E/kT = 1.44$ and $g/(kT) = -0.666$.

Conclusions

In the present work, we have shown using a very simple model, based on statistical mechanics, that the controversial origin of the entropy step between stage II and stage I for lithium intercalation in graphite may be explained on a configurational basis, in agreement with the conjecture of Yazami and Reynier[18] concerning the occurrence of a dilute lithium layer between adjacent complete lithium hexagonal layers.

Another important result is that the interaction between intercalated ions can be inferred to be strongly attractive, as was assumed by Levi et al.[22] when simulating voltammetric profiles.

Acknowledgments

This work was supported by PIO Conicet-YPF 3855/15, PID Conicet-11220110100992, PID Conicet-11220150100624 , Program BID-Foncyt (PICT-2012-2324, PICT-2015-1605), SeCyT of the Universidad Nacional de Córdoba and YPF-Tecnología (Y-TEC), Argentina. This work was performed at INFIQC-IFEG-CONICET and Facultad de Ciencias Químicas, FaMAF, Universidad Nacional de Córdoba, Argentina.

References

1. D. In Choi, G.-B. Han, D. Jin Lee, J.-K. Park, and J. Wook Choi, *Journal of The Electrochemical Society*, **158**, A1150 (2011).
2. O. Jankovský, J. Kovaík, J. Leitner, K. Rika, and D. Sedmidubský, *Thermochimica Acta*, **634**, 26 (2016).
3. A. Kvasha, I. Urdampilleta, I. de Meatza, M. Bengoechea, J. A. Blázquez, L. Yate, O. Miguel, and H.-J. Grande, *Electrochimica Acta*, **215**, 238 (2016).
4. M. Takahashi, H. Ohtsuka, K. Akuto, and Y. Sakurai, *Journal of The Electrochemical Society*, **152**, A899 (2005).
5. H. Ge, T. Hao, B. Zhang, L. Chen, L. Cui, and X.-M. Song, *Electrochimica Acta*, **211**, 119 (2016).
6. H. ping Liu, G. wu Wen, S. fu Bi, C. yu Wang, J. min Hao, and P. Gao, *Electrochimica Acta*, **192**, 38 (2016).
7. T. Deng and X. Zhou, *Journal of Solid State Electrochemistry*, **20**, 2613 (2016).
8. K. Dai, Z. Wang, G. Ai, H. Zhao, W. Yuan, X. Song, V. Battaglia, C. Sun, K. Wu, and G. Liu, *Journal of Power Sources*, **298**, 349 (2015).
9. J. Hong, H. Maleki, S. Al Hallaj, L. Redey, and J. R. Selman, *Journal of The Electrochemical Society*, **145**, 1489 (1998).
10. C. Heubner, M. Schneider, C. Lämmel, and A. Michaelis, , *Electrochimica Acta* **186**, 404 (2015).
11. S. Abada, G. Marlair, A. Lecocq, M. Petit, V. Sauvant-Moynot, and F. Huet, *Journal of Power Sources*, **306**, 178 (2016).
12. Y. Reynier, R. Yazami, and B. Fultz, *Journal of Power Sources*, **119**, 850 (2003).
13. Y. F. Reynier, R. Yazami, and B. Fultz, *Journal of The Electrochemical Society*, **151**, A422 (2004).
14. S. R. Cain, W. Infantolino, A. Anderson, E. Tasillo, and P. Wolfgramm, *Electrochimica Acta*, **185**, 250 (2015).
15. H. Yang and J. Prakash, *Journal of The Electrochemical Society*, **151**, A1222 (2004).
16. P. J. Osswald, M. del Rosario, J. Garche, A. Jossen, and H. E. Hoster, *Electrochimica Acta*, **177**, 270 (2015).
17. J. P. Schmidt, A. Weber, and E. Ivers-Tiffée, *Electrochimica Acta*, **137**, 311 (2014).
18. R. Yazami and Y. Reynier, *Journal of Power Sources*, **153**, 312 (2006).
19. B. Fultz, *Progress in Materials Science*, **55**, 247 (2010).
20. E. M. Perassi and E. P. Leiva, *Electrochemistry Communications*, **65**, 48 (2016).
21. See for example Chapter 2 of T. L. Hill, *An Introduction to Statistical Thermodynamics*, Addison-Wesley Publishing Company, Inc, London, 1960.
22. M.D. Levi and D. Aurbach, *Journal of Electroanalytical Chemistry*, **421**, 79 (1997).
23. See for example Chapter 14 of T. L. Hill, *An Introduction to Statistical Thermodynamics*, Addison-Wesley Publishing Company, Inc, London, 1960.
24. J.-S. Filhol, C. Combelles, R. Yazami, and M.-L. Doublet, *J. Phys. Chem. C*, **112**, 3982 (2008).